MODIFIED WEIGH FUNCTION IN BACKPROJECTION METHOD

Joyce da Silva Bevilacqua[1,2]
[1] Centro Universitário Senac – Campus Santo Amaro. Av. Eng. Eusébio Stevaux, 823, 04696-000, São Paulo, SP, Brasil.
joyce.bevilacqua@sp.senac.br
[2] Instituto de Matemática e Estatística da Universidade de São Paulo.
Rua do Matão, 1010, 05508-900, São Paulo, SP, Brasil.
joyce@ime.usp.br
Elisa Pereira Kameda
Instituto de Matemática e Estatística da Universidade de São Paulo.
Rua do Matão, 1010, 05508-900, São Paulo, SP, Brasil.
ekameda@linux.ime.usp.br

Abstract. *Internal conductivity distribution of a slice of the thorax can be determined by a reconstruction method that projects values of voltages measured on the boundary into the domain, weighted by a function that depends on the current applied in the boundary. In the classical model the projection path and the weigh function are defined by the dipole model in homogeneous medium. However, because of the ill-posed nature of the problem objects loose focus, collapse or have their maximal conductivity value reduced approximately by 16% when moved from a position near the boundary to the centre of the domain. The goal of this work is to improve the quality of reconstructed images, introducing two new weigh functions. One based on the exponential function and other on polynomial interpolation. Both have their parameters modified in order to fit a pre-defined outline, that defines in advance the region of the domain that must be improved. Tests were applied to two different experimental data. A circular tank filled with saline solution, where one cylinder is introduced inside and other when two cylynders of different size and position are introduced inside. Comparison between original and reconstructed images using these new weigh functions shows that is possible to separate collapsed regions and also improve the value of maximal conductivity inside the domain, by an appropriate definition of the outline .*

Keywords*: backprojection, image reconstruction, impedance, tomography, interpolation*

1. Electrical impedance tomography

During the evolution of a respiratory disease, lungs dynamic at alveolar level can be monitored only by a few numbers of X-ray or computerized tomography images. Side effects of radiation and difficulties in transportation of the patients are significant restrictions to these techniques. Non-invasive and portability aspects must be considered for medical application.

Electrical impedance tomography is based on the electrical properties of materials. As different materials have different electrical properties it is possible to identify the location of each one by calculating their conductivity (Cheney, Isaacson and Newell,1999). To obtain an image of a closed region Ω electrical currents are applied and voltages measured in pairs of electrodes attached to the boundary $\partial\Omega$ and reconstruction algorithms developed to obtain the internal conductivity for each point inside the region.

Consider N electrodes positioned at the contour of the thorax and currents of 1 mA successively applied in pairs of electrodes. For each injection pair, voltages are measured in all the electrodes and an image, that represents a slice of the thorax at an instant in the respiratory cycle, is obtained after a complete set of measurements. For medical application, the advantages of this technique are the non invasive characteristic and portability. However these advantages are counterbalanced with low resolution of the images.

The image quality is limited by the number of independent measurements, signal to noise ratio, skin-electrode contact impedance and error propagation in numerical algorithm. The central region of the domain is poorly reconstructed because of the ill-posed nature of the problem and also the difficulty of electrical currents to reach this region. Objects loose focus, collapse or have the maximal value of conductivity reduced approximately by 16% if they go from a position near the boundary to the centre of the domain. Uniqueness of the solution is not guaranteed because of the finite number of independent measurement that could be obtained at the boundary (Borcea, 2002).

The algorithm used to reconstruct the image in this work is the backprojection where the values of voltages in the boundary are projected trough the potential lines defined by the dipole mode (Herman, 1980). The idea of the algorithm is very simple and is represented by Fig. 1: electrical current of 1 mA is applied in a pair of electrodes e_1-e_2 modeled as two equal charges with opposite signals. The dipole is located in d and potential and lines of currents are represented, respectively, by the blue and green lines. The red line is a potential that passes through a specific point x inside the domain. In the classical implementation the projection is weighted by a function proportional to the lines of currents (Santosa and Vogelius, 1990). The dipole location is a singular point so the weight function goes from infinity through zero proportional to the inverse of the distance $dist(x,d)$, where x is a point inside the domain and d the dipole location.

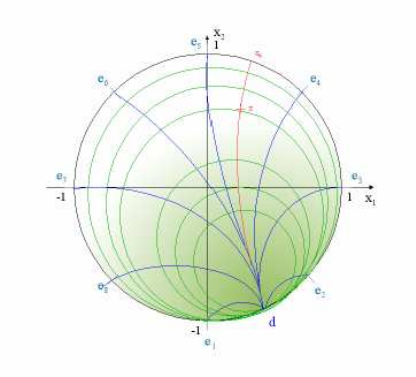

Figure 1. Potential and lines of currents of the dipole

The classical weight function is shown in Fig. 2 for one single pair of electrodes that defines the dipole *d*. The decay of this weight function from infinity to zero is very fast, being effectively different from zero only in a ring near the boundary. As the injection pair rotates the projection in the central region is almost neglected. The opposite occurs with the region near the dipole. In this region the weight has a high value – infinity – but the signal to noise ratio in measured values of voltages near the injection pair is also high. So, with this weight function the information near the center is neglected and the opposite occurs with points near the dipole, even being wrong.

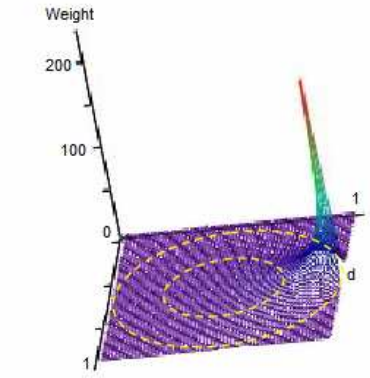

Figure 2. Weight function for the classical backprojection

The goal of this work is to improve the quality of reconstructed images, introducing new weigh functions with the intention to recover some lost information in the central region. Two different functions are defined: one is based on the exponential function and other on polynomial interpolation.

In the next sections the classical and the new weight functions will be constructed and compared.

2. Weight functions

In the classical implementation of the backprojection (Barber and Brown, 1984) is assumed that if the distance of the electrodes is small if compared with distances of points inside the domain Ω, the electrical field can be approximated by the one generated by two charges of same value and opposite signals. The mathematical model is given by Maxwell´ s equation for a dipole in a homogeneous medium located between the pair of electrodes.

$$\begin{cases} \nabla.\gamma\nabla u = 0, \ \ in\,\Omega \\ \gamma.\dfrac{\partial u}{\partial \vec{n}} = \vec{j}, \ \ on\,\partial\Omega, \end{cases} \tag{1}$$

where, γ is the conductivity, u the voltage, $\vec{j}$ the applied electrical current, $\vec{n}$ the normal vector, Ω and $\partial\Omega$, respectively the domain and the boundary.

The calculation of the conductivity distribution γ knowing the electrical current and the voltages at the boundary is called inverse problem. An important remark is about the uniqueness of the solution. The voltage-to-current (Dirichlet-

to-Neumann) map is unique only if the data at the boundary is a continuous function (Calderón, 1980). For a configuration of N electrodes, which is used in this paper, the adjacent configuration gives N(N-3)/2 independent measurements, taking into account the reciprocity theorem and not considering the voltages measured involving the injection pair (Tang et al., 2002).

The model defined in Eq.(1) is approximated by a linear model assuming that a small perturbation $\delta\gamma$ in the conductivity distribution corresponds to a small perturbation δu in the values of the boundary voltages. In this formulation the reconstructed images represent the variation of conductivity relative to a homogeneous medium assumed to be $\gamma = 1$ and the variation $\delta\gamma$ is null near the dipole to avoid the singularity effect. The domain is defined as the unitary circle. Equation (2) represents the linear model and establishes a connection between the known solution of the homogeneous and the perturbed problem.

$$\begin{cases} \nabla.(\gamma\nabla(\delta u)) = -\nabla.(\delta\gamma.\nabla u), \ in\ \Omega \\ \gamma\dfrac{\partial(\delta u)}{\partial\vec{n}} = -\delta\gamma\dfrac{\partial u}{\partial\vec{n}}, \ on\ \partial\Omega, \end{cases} \tag{2}$$

Measuring the difference of voltages δu at the boundary the variation of conductivity $\delta\gamma$ is calculated by Eq. (2). Therefore, considering *N* the total number of electrodes in the boundary, for each drive pair, backprojection algorithm projects the boundary voltage perturbation through the potential lines defined by the dipole. As the current is applied in turn in all pairs of electrodes, the final image is a composition of *N* back propagated information each one related to one dipole. With the introduction of these restrictive hypothesis the electric field $\vec{E}$ is derived by a potential *u*

$$\vec{E} = -\nabla u \tag{3}$$

being *u* the superposition of two fields each one defined by each charge

$$u(x) = u_+(x) + u_-(x) \tag{4}$$

The potential is the first order Taylor approximation, around a small parameter defined as the distance between the charges, and the expansion is made in complex variables. Being (x_1, x_2) the coordinates of a point *x* inside the domain, the potential *u* is defined by

$$u(x) = U(x) + V(x) \tag{5}$$

where

$$U(x) = \frac{x_1}{{x_1}^2 + {x_2}^2}, V(x) = \frac{x_2}{{x_1}^2 + {x_2}^2}\ , \tag{6}$$

$x_1 = \omega^{\perp} x$, $x_2 = 1 - \omega x$, $\omega = (\omega_1, \omega_2)$ is the dipole position and $\omega^{\perp} = (-\omega_2, \omega_1)$.

The backprojection is implemented by the integral

$$B(x) = -\frac{1}{2\pi}\int_{\|\omega\|=1} W(u_\omega(x), \omega)\Phi(x, \omega)dS_\omega \tag{7}$$

where, $x \in \Omega$ and the integral is calculated relative the dipole position ω and the function *W*, is given by

$$W(u_\omega(x), \omega) = -\frac{\dfrac{\partial(\delta u(S, \omega))}{\partial\tau}}{\dfrac{\partial u(S, \omega)}{\partial\tau}} \tag{8}$$

where, δu is the potential variation between the perturbed and reference medium and *u* the potential of the reference medium (homogeneous).

2.1. Classical weight function

The function V is the harmonic conjugate to $-U$ in Ω and

$$x = (x_1, x_2) \rightarrow (-U, V) \tag{9}$$

maps the unitary circle in the superior semi-plane $P = \{ V > ½\}$ as shown in Fig. 3

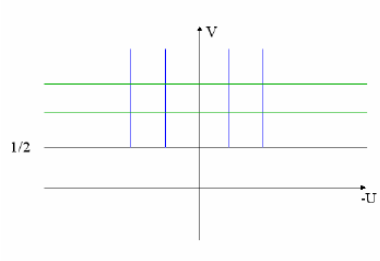

Figure 3. Map of the unitary circle into the superior semi-plane.

The weight function Φ deduced by the classical formulation, for a dipole ω is given by

$$\Phi(x, \omega) = 2V(x, \omega) - 1 \tag{10}$$

2.2. New weight function

In this work we introduce new weight function in order to avoid the singularity near the dipole and also include some information from the central region. Two types were defined and tested, one based on the exponential behavior of the original function Φ_e and other Φ_p constructed by polynomial interpolation.

The function Φ_e depends on four parameters, α, β, a and b.

$$\Phi_e = (\alpha + \beta x).exp(a + bx) \tag{11}$$

The identification of the interval of variation of each parameter was detected by experimental simulation and none restriction were imposed to them in advance. The minimum and maximum values were defined observing the degeneration of the reconstructed image. As a control image we use experimental data of one tank filled with saline solution representing the homogeneous problem and two different non-homogeneous problems, respectively, a unique cylinder and two cylinders of different size were positioned inside the tank.

The weight function Φ_p is constructed based on a desired profile which is chosen by an interactive interface shown in Fig. 4. The potential lines still remain given by the dipole model, but the distance between the dipole and the boundary of a potential line was normalized by 1 to assure the same weight at the same proportional distance.

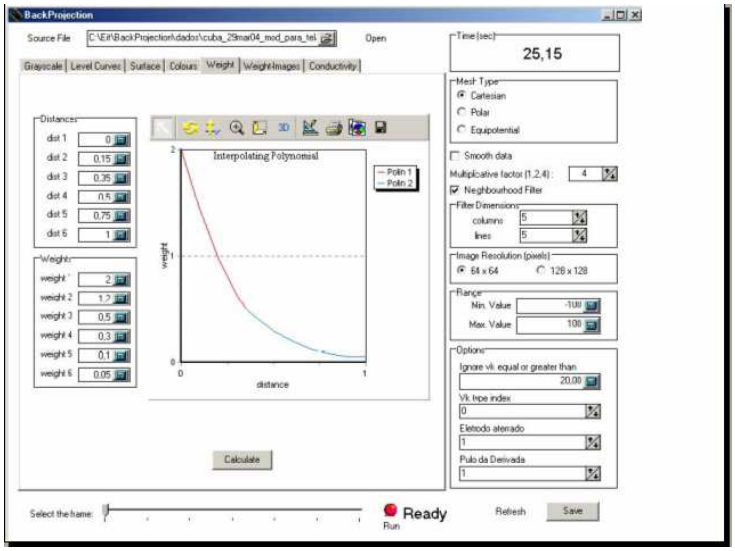

Figure 4. Interactive interface to design the profile of the weight function

The two columns in the left define the points (P_u, P_Φ) where the interpolation will be done. In the upper column the values of P_u that is chosen in the interval [0,1] and in the lower one the position P_Φ which defines a local weight. In Fig.4 the profile is quite similar the classic function, but the interface gives total freedom to define any wanted path.

As in the case of the exponential weight function the image degeneration is used to classify the polynomial weight function too. In next section some results were shown.

3. Results

All the simulations used experimental data. The homogeneous data is obtained by a circular tank, with 30cm of diameter, filled with saline solution. The non-homogeneous cases, cylinders of different sizes and number were positioned inside the tank, filled with the same solution. The test images used in this work are given by Fig. 5. Normalizing the radius of the tank equal to 1, the 1-cylinder test has radius 0.1 positioned at (0.01,-0.6) assuming Cartesian coordinates in the centre of the cylinder. The 2-cylinder test the radius and position of the cylinders are defined as C1={0.1, (0.01, -0.75)} and C2 = {0.05, (0.0)}.

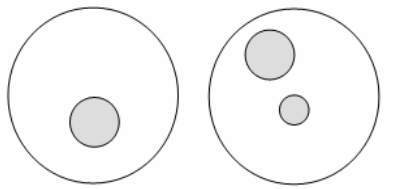

Figure 5. Reference images for the reconstruction algorithm

3.1. Reconstructions using the weight function Φ_e

Results obtained with the weight function Φ_e are affected by the linear terms in the sense that only values of β and a near zero do not degenerate the image. So, the parameters β and a, were defined equal to zero the image degenerates and the weight function is given by

$$\Phi_e = \alpha.exp(bx) \tag{12}$$

For one cylinder case a classification of the reconstructed image is defined in Tab. 1, for different values of α and b, following the notation: *P* for well defined cylinder in the correct position, *D* for degenerate image, *O* for oscillatory behavior inside the domain, *OB* oscillatory behavior in the boundary.

Table 1. Quality of reconstructed image for different parameters of Φ_e and one cylinder case, assuming $\beta = a = 0$.

b \ α	-0.5	0.5	1.0	2.0
-2.5	*D*	*D*	*D*	*D*
-1.25	*P+O*	*P+O*	*P+O*	*P+O*
-0.75	*P+O*	*P+O*	*P+O*	*P+O*
-0.625	*P+O*	*P+O*	*P+O*	*P+O*
-0.5	*P+O*	***P***	*P+O*	*P+O*
-0.313	*P+O*	***P***	*P+O*	*P+O*
-0.156	*P+OB*	***P***	*P+O*	*P+O*
-0.078	*P+OB*	*P+OB*	*P*	*P+O*
-0.062	*P+OB*	*P+OB*	*P+OB*	*P*
0.156	*P+OB*	*P+OB*	*P+OB*	*P+OB*
0.313	*D*	*D*	*D*	*D*

For $b \leq -1.25$ or $b \geq 0.313$ the image is degenerate independent of α. The cylinder position is recovery with oscillatory behavior inside or on the boundary between these values, being the best images given by $\alpha = 0.5$ and $-0.5 \leq b \leq -0.156$. Figure 6 shows the reconstructed image for three different parameters of Φ_e. Fixing $\alpha = 0.5$ the sequence shows values of $b = -1.25$, $b = -0.313$ and $b = 0.156$ from the left to the right, respectively. For the same order the values of the maximal amplitude for each image is 0.06, 0.188 and 0.109 showing that the best image corresponds to the

parameters $\alpha = 0.5$ and $b = -0.313$. A similar study was made with two cylinders inside the domain. Table 2 shows the result. The notation is the same, including the second *P* for the second cylinder. The lower cases for *o* and *p* represent, respectively, small oscillation and amplitude of the maximal value for one of the cylinders.

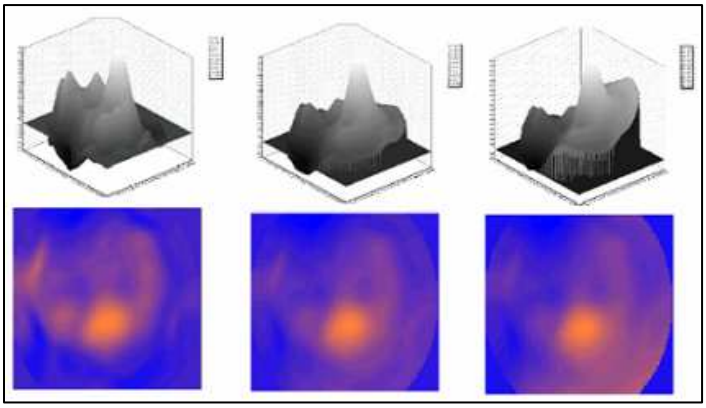

Figure 6. Sequence of reconstructed images of one cylinder inside the domain using Φ_e.

Table 2. Quality of reconstructed image for different parameters of Φ_e - two cylinder case.

b \ α	0.5	1.0	2.0
-2.5	*PP+o*	*PP+o*	*PP+o*
-1.25	*PP+O*	***PP***	***PP***
-0.625	*Pp+O*	*Pp+o*	*Pp+o*
-0.313	*Pp+O*	*Pp+O*	*Pp+O*
-0.156	*D*	*D*	*D*
-0.078	*D*	*D*	*D*
0.313	*D*	*D*	*D*

From Tab.2 we conclude that better results are given by $b = -1.25$ and $1.0 \leq \alpha \leq 2.0$. Figure 7 shows the reconstructed image for two different parameters (α, b), respectively, from the left to the right {1.0, -1.25} and {1.0, 0.313}. For the same order the absolute values of maximal amplitude for the cylinders are {0.138, 0.036} and {0.959, 0.014}, corresponding the second term for the central object. From the 2D image is possible to detect both cylinders but is very difficult to recover information from the center of the image.

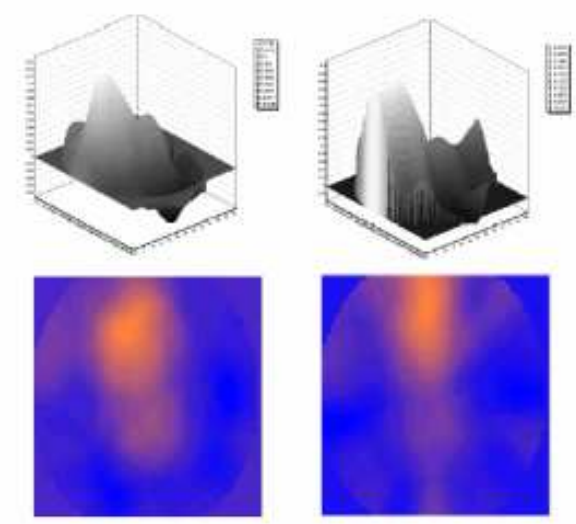

Figure 7. Reconstructed images of two cylinders inside the domain using Φ_e.

3.2. Reconstructions using the weight function Φ_p

The free way to define the weight function Φ_p by the interpolating polynomial is an advantage because of the possibility to explore different profiles in very simple way. The partition $\wp$ of the interval [0,1] is composed by 6 points, not necessarily equally spaced. To be possible the comparison between different polynomials the partition is the same for all simulations $\wp = \{0.001, 0.15, 0.35, 0.5, 0.75, 1.0\}$. In Fig. 8 four different interpolating functions from the left to the right Φ_{p1}, Φ_{p2}, Φ_{p3}, Φ_{p4} are shown. Φ_{p1} is similar to the classical weight function but in this case there is no singularity at the dipole position and the decay can be less abrupt.

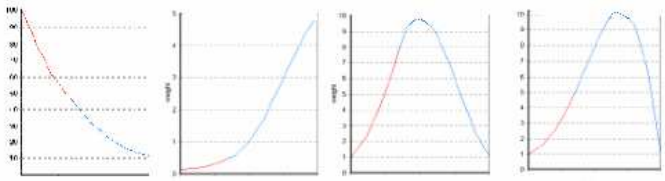

Figure 8. Four weight functions defined by polynomial interpolating.

Fixing the partition $\wp$ Tab.3 shows two sets of interpolation points for each weight function Φ applied to experimental data. The columns Position identify the centre of the reconstructed cylinder, conductivities columns show the maximal and minimal values reconstructed for conductivity. Figure 9 shows the 8 corresponding reconstructed images. Except by the polynomial function Φ_{p1}, degeneration is almost observed in the other profiles and small variations in the weights can produce the same class of image but significant changes in the values of conductivity.

Table 3. Classification of the image of one cylinder reconstructed by the functions Φ_{p1}, Φ_{p2}, Φ_{p3}, Φ_{p4}

Weight	Image		Values of P_Φ						Position		conductivity		quality
		$\wp$	0.001	0.15	0.35	0.5	0.75	1.0	x	y	Max γ	Min γ	
$\Phi_{p1}(P_u)$	1a		5	3	1	0.5	0.2	0.45	0.15	-0.5	0.016	0.011	P
	1b		100	70	45	30	15	10	0.15	-0.4	0.585	0.417	P
$\Phi_{p2}(P_u)$	2a		1	4	10	17	30	40	0.2	-0.9	0.397	0.288	PO
	2b		0.25	0.5	2	4	7	10	-	-	0.406	0.005	D
$\Phi_{p3}(P_u)$	3a		5	15	30	40	25	5	-	-	0.545	0.019	D
	3b		1	3	8	10	6	1	0.15	-0.6	0.132	0.095	P
$\Phi_{p4}(P_u)$	4a		10	11	17	35	40	10	-	-	0.547	0.392	D
	4b		1	2	5	8	10	1	0.15	-0.65	0.13	0.093	P

The weight Φ_{p2} produces almost degenerate images, because the weight is approximately zero near the dipole where the information is more accurate. If the image is not degenerate the centre of the reconstructed object has no significant change for Φ_{p3}, Φ_{p4} but for Φ_{p1} is observed a significant change in the position. The maximal conductivity increases in all these three cases even if the object is near the centre of Ω or when more than one object is inside the tank.

4. Conclusion

Two different weight functions were used in the backprojection method: one is based on the exponential function and other on polynomial interpolation. The study involving the exponential weight shows that it is quite difficulty to find a set of parameters able to improve the image. Best results were observed with the polynomial function.

Different profiles were tested in the backprojection method for a polynomial weight function. For some Φ_{p3}, Φ_{p4}, the value of maximal conductivity increases without changing the position of the object. For Φ_{p1} maximal conductivity increases but the position of the object is not maintained.

With the profile control of the weight function is possible to improve the maximal value of conductivity avoiding regions near the dipole and adding the contribution of internal regions.

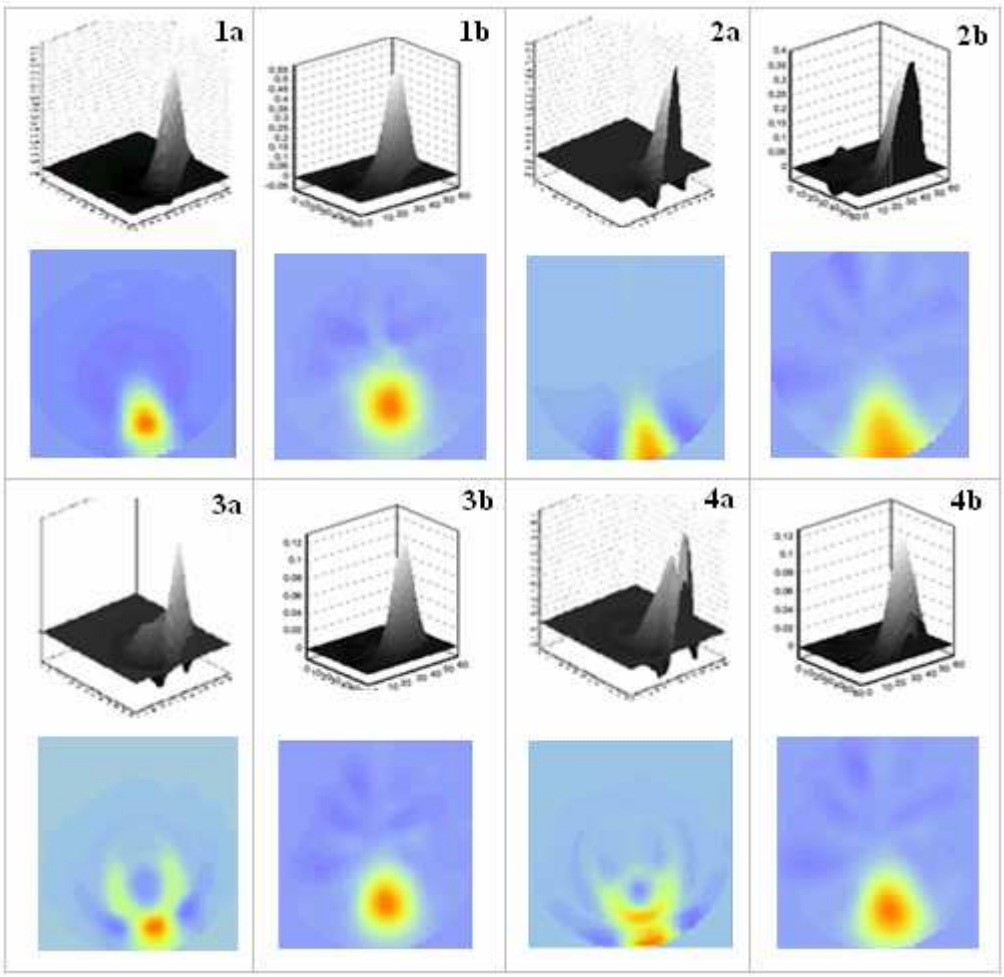

Figure 9. Reconstruction of the sequence Φ_{p1}, Φ_{p2}, Φ_{p3}, Φ_{p4}.

5. Acknowledgements

The numerical calculations were performed using computing equipment supported by FAPESP under grant number 2001/05303-4 and scholarship FAPESP 03/01439-4.

6. References

Borcea, L.,2002, “Electrical impedance tomography”, Inverse Problems 18, R99 - R136 (2002).

Barber, D.C., Brown, B.H., 1984, “Applied Potential Tomography”, *J. Phys. E: Sci. Instrum.*, Vol. 17, pp 723-733.

Calderón, A. P., 1980, “On an inverse boundary value problem”, Seminar on Numerical Analysis and its applications to Continuum Physics, Rio de Janeiro, pp. 65-73.

Cheney, M., Isaacson, D., Newell, J.C.,1999, “Electrical Impedance Tomography”, *SIAM Review*, Vol.41 (1), pp.85-101.

Santosa, F., Vogelius, M, 1990, “A backprojection algorithm for electrical impedance image”, SIAM J. Appl. Math., Vol. 50, No. 1, pp. 216–243.

Herman, G.T., 1980, “Image Reconstruction from Projections”, Computer Science and Applied Mathematics, Werner Rheinboldt, Academic Press, New York.

Tang, M., Wang, W., Wheeler, J., McCormick, M., Dong, X., 2002, “The Number of Electrodes and Basis Functions in EIT” , *Physiol. Meas.* Vol 23, pp. 129-140.

6. Responsibility notice

The authors are the only responsible for the printed material included in this paper.